Supplemental Figure Legends

Figure S1. Common and differentially essential genes under ammonia or BafA1 treatments**,** Related to Figure 1.

(A) Plot of gene essentiality scores (DepMAP) of v-ATPase subunits.

(B) Gene scores in untreated versus NH_4Cl-treated (3mM) KMS26 cells (top). The gene score is the median log2 fold change in the abundance of all sgRNAs targeting that gene during the culture period. Most genes, as well as non-targeting control sgRNAs, have similar scores in the presence or absence of the treatments. Top 20 genes scoring as differentially required upon ammonium chloride treatment (bottom). Genes associated with iron homeostasis are in purple, central carbon metabolism in blue, and cholesterol synthesis in red.

(C) Guide score plots for guides targeting *SLC12A9* in NH_4Cl (top) and BafA1 (bottom) negative genetic screens.

(D) Fold change in cell number (log2) of untreated (gray) or NH_4Cl (4mM) treated (blue) parental or cells expressing two different guides targeting *SLC12A9* under treatment for 5 days (mean ± SD, n=3).

(E) Guide score plots for guides targeting *ATP6V0A2* in NH_4Cl (top) and BafA1 (bottom) negative genetic screens.

(F) Fold change in cell number (log2) of untreated (gray) or BafA1 (3nM) treated (blue) parental or cells expressing two different guides targeting *ATP6V0A2* under treatment for 5 days (mean ± SD, n=3).

Figure S2. Under lysosomal dysfunction, cells require cholesterol synthesis and iron import, Related to Figure 2.

(A) Immunoblot analysis for indicated proteins of SLC11A2 knockout Jurkat cells. GAPDH was used as a loading control.

(B) NB-598-mediated inhibition of SQLE using a small molecule inhibitor (NB-598) is synthetic lethal with lysosomal pH disruption in HeLa and 293T cell lines. Fold change in cell number (log2) of untreated or NB-598 (10μM) treated cells under BafA1(3nM) for 5 days (mean ± SD, n=3, **p<0.05).

(C) DFO-mediated iron chelation is synthetic lethal with lysosomal pH disruption in mouse KP pancreas, HeLa, and 293T cell lines. Fold change in cell number over 5 days (log2) of untreated or DFO (5μM) treated cells under BafA1(3nM). (mean ± SD, n=3, **p<0.05).

(D) DFO-mediated iron chelation is synthetic lethal with the lysosomotropic drug, Chloroquine. Fold change in cell number over 5 days (log2) of untreated or DFO (10μM) treated cells under CQ (20μM) (mean ± SD, n=3, **p<0.05).

(E) Immunoblotting for the indicated iron sulfur cluster containing proteins in the absence or presence of BafA1 (10nM) and/or free cholesterol supplementation (5μg/ml). GAPDH and Beta-actin are used as a loading controls.

Figure S3. Modulating cellular iron enables proliferation under lysosomal dysfunction, Related to Figure 3.

(A) Cholesterol supplementation does not rescue anti-proliferative effects of Bafilomycin A1. Fold change in cell number (log2) of Jurkat cells in the absence and presence of free cholesterol (5μg/ml) after treatment with lipoprotein depleted serum (left) or full serum (right) for 5 days (mean ± SD, n=3, **p<0.05). In the full serum condition, cells were treated with or without BafA1(5nM) for the 5 days.

(B) Ferrostatin-1 supplementation alone does not rescue anti-proliferative effects of Bafilomycin A1. Fold change in cell number (log2) of 293T and mouse pancreas cancer cells cultured in the absence and presence of ferrostatin (1μM) for 5 days.
(C) Illustration of relative enrichment of SLC11A2 isoforms 1 or 2 for lysosomal or plasma membranes, respectively.
(D) In KP pancreas mouse cells, expression of SLC11A2.2 but not SLC11A2.1 is sufficient to rescue high dose BafA1 toxicity corresponding to Figure 3D. Fold change in cell number (log2) of untreated or BafA1 treated cells expressing, empty vector or SLC11A2 isoform 1 or isoform 2 (mean ± SD, n=3, **p<0.05).
(E) In Jurkat cells, expression of SLC11A2 potentiates iron rescue (0.1mg/ml) of BafA1 toxicity (mean ± SD, n=3, **p<0.05).

Figure S4. Cellular processes that are affected by iron rescue of lysosomal dysfunction, Related to Figure 4 and Figure 5.
(A) Heat maps of mean whole cell and lysosomal metabolite abundances of BafA1 treated or combination BafA1 and FAC treated cells corresponding to Figure 4A.
(B) Immunoblots of pS6K and S6K as a readout of mTOR reactivation following amino acid starvation and feeding under indicated BafA1 concentrations in cells preincubated for 24 hours in the presence or absence of FAC (0.4mg/ml).
(C) Immunoblotting for the indicated iron response pathway proteins. GAPDH is used as a loading control.
(D) Pyruvate does not rescue anti-proliferative effects of Bafilomycin A1. Fold change in cell number (log2) of Jurkat cells grown in the absence or presence of BafA1 (5nM) and/or pyruvate (2mM) for 5 days (mean ± SD, n=3).
(E) Blue Native PAGE and immunoblotting for components of Complex I (GRIM19), Complex II (SDHB), or Complex IV (COX4) to measure respective stabilities.

Figure S5. Pyruvate derived citrate is essential upon cellular iron depletion, Related to Figure 6.
(A) Gene scores in untreated versus DFO-treated (2μM) Jurkat cells (top). The gene score is the median log2 fold change in the abundance of all sgRNAs targeting that gene during the culture period. Most genes, as well as non-targeting control sgRNAs, have similar scores in the presence or absence of the treatments. Top 20 genes scoring as differentially required upon DFO treatment (bottom). Genes associated with iron homeostasis are in purple and central carbon metabolism in blue.
(B) Guide score plots for guides targeting *PDHA1* (top) and *PDHB* (bottom) in DFO negative genetic screen.
(C) Immunoblot analysis for indicated proteins of PDHB knockout Jurkat cells. GAPDH was used as a loading control.
(D) Fold change in cell number (log2) of parental and PDHA1 null Jurkat cells in the absence and presence of BafA1 (3nM) (top) and ammonia (5mM) (bottom) for 5 days (mean ± SD, n=3, **p<0.05).
(E) Fold change in cell number (log2) of parental, PDHB null and SQLE null Jurkat cells grown for 5 days in media containing 10% FBS or 10% lipoprotein depleted serum. (mean ± SD, n=3, **p<0.05).
(F) Fold change in cell number (log2) of parental and PDHB null cells cultured in the absence or presence of Sodium Citrate (10mM) and indicated concentrations of BafA1 grown for 5 days (mean ± SD, n=3, **p<0.05).
(G) Fractional labeling of citrate, alpha-ketoglutarate, fumarate, and malate from U^{13}C-Glucose in wild type and PDHB null Jurkat cells. Related to figure 4C.

(H) Relative metabolite abundance of citrate labeling from $U^{13}C$-Glucose (mean ± SD, n=3, **p<0.05).

Figure S6. Characterizing the downstream functions of citrate**,** Related to Figure 6.

(A) Cellular ROS levels assessed by flow cytometry measuring CellRox deep red fluorescence. Histogram plots of fluorescence intensity in WT and PDHB_KO Jurkat cells following 24h BafA1 (10nM) treatment. 30-minute treatment with TBHP (200μM) was used to induce cellular ROS as a positive control.

(B) Antioxidants supplementation does not rescue PDHB_KO sensitivity to Bafilomycin A1. Fold change in cell number (log2) of Jurkat cells grown in the absence or presence of BafA1 (2nM) and/or antioxidants Ferristatin-1 (1μM), Trolox (100μM), or GSH (1mM) for 5 days (mean ± SD, n=3) (top).

(C) Fractional labeling of palmitate in WT and PDHB_KO cells from $U^{13}C$-Glucose.

Figure S1

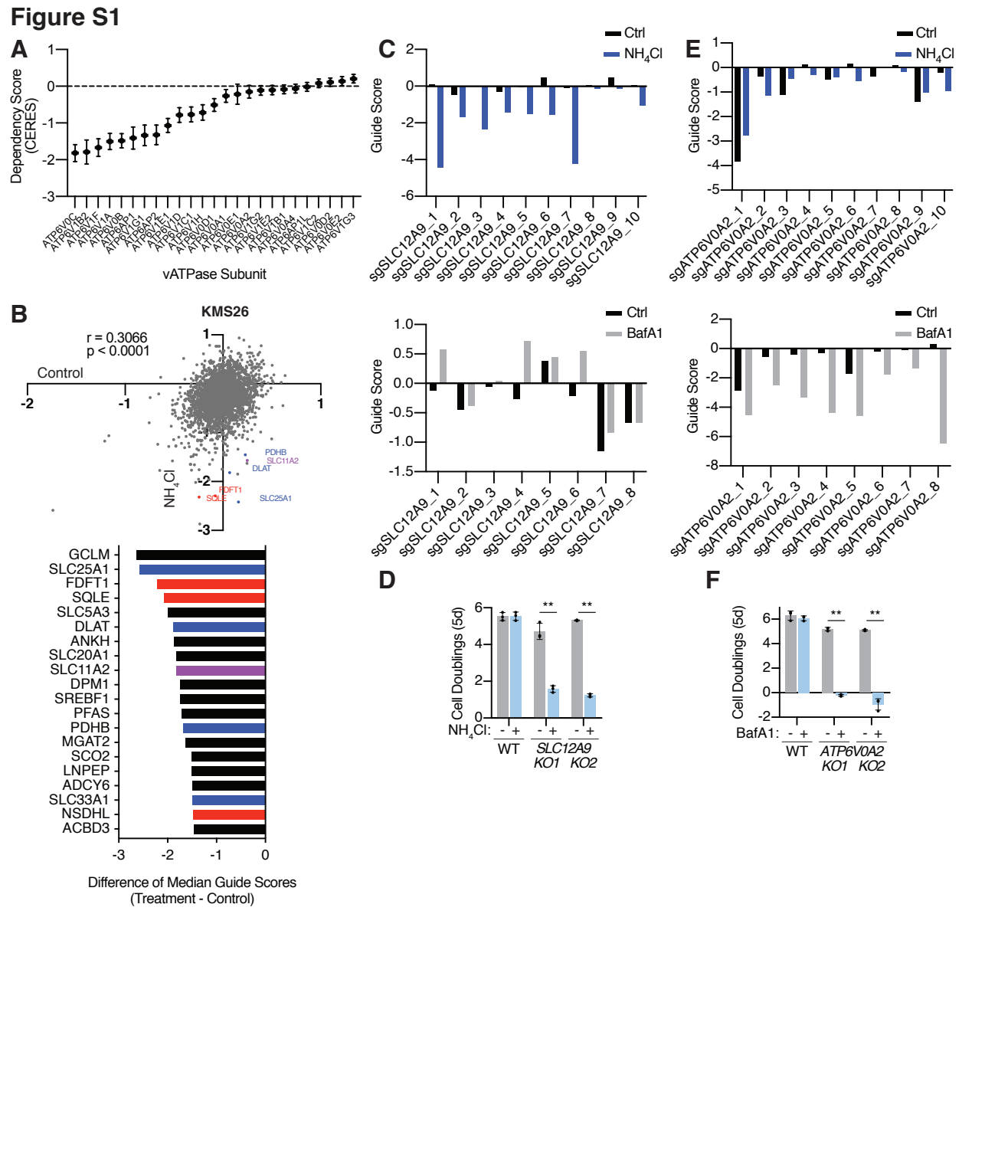
A
Dependency Score (CERES)
vATPase Subunit
B
KMS26
r = 0.3066
p < 0.0001
Control
NH4Cl
PDHB
SLC11A2
DLAT
FDFT1
SQLE
SLC25A1
GCLM
SLC25A1
FDFT1
SQLE
SLC5A3
DLAT
ANKH
SLC20A1
SLC11A2
DPM1
SREBF1
PFAS
PDHB
MGAT2
SCO2
LNPEP
ADCY6
SLC33A1
NSDHL
ACBD3
Difference of Median Guide Scores
(Treatment - Control)
C
Ctrl
NH4Cl
Guide Score
sgSLC12A9_1
sgSLC12A9_2
sgSLC12A9_3
sgSLC12A9_4
sgSLC12A9_5
sgSLC12A9_6
sgSLC12A9_7
sgSLC12A9_8
sgSLC12A9_9
sgSLC12A9_10
E
Ctrl
NH4Cl
Guide Score
sgATP6V0A2_1
sgATP6V0A2_2
sgATP6V0A2_3
sgATP6V0A2_4
sgATP6V0A2_5
sgATP6V0A2_6
sgATP6V0A2_7
sgATP6V0A2_8
sgATP6V0A2_9
sgATP6V0A2_10
Ctrl
BafA1
Guide Score
sgSLC12A9_1
sgSLC12A9_2
sgSLC12A9_3
sgSLC12A9_4
sgSLC12A9_5
sgSLC12A9_6
sgSLC12A9_7
sgSLC12A9_8
Ctrl
BafA1
Guide Score
sgATP6V0A2_1
sgATP6V0A2_2
sgATP6V0A2_3
sgATP6V0A2_4
sgATP6V0A2_5
sgATP6V0A2_6
sgATP6V0A2_7
sgATP6V0A2_8
D
Cell Doublings (5d)
NH4Cl:
WT
SLC12A9 KO1
SLC12A9 KO2
F
Cell Doublings (5d)
BafA1:
WT
ATP6V0A2 KO1
ATP6V0A2 KO2

Figure S2

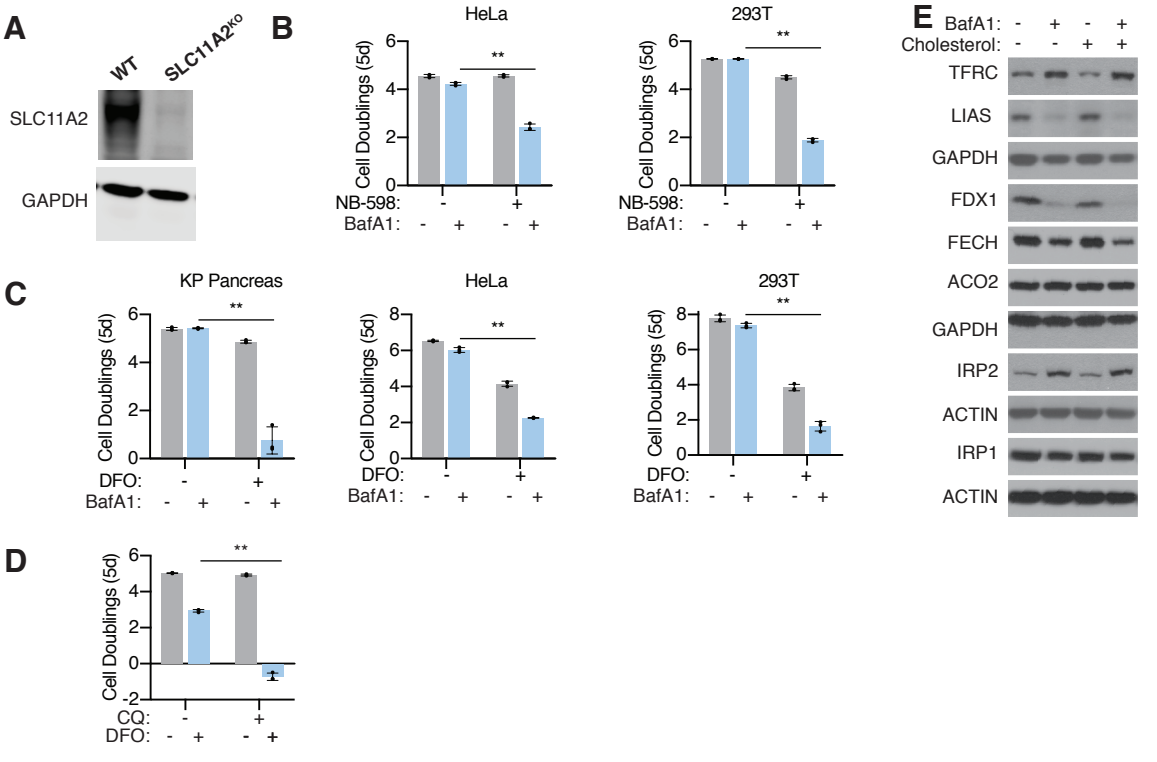
A
WT
SLC11A2ko
SLC11A2
GAPDH
B
HeLa
293T
Cell Doublings (5d)
NB-598:
BafA1:
C
KP Pancreas
DFO:
D
CQ:
E
BafA1:
Cholesterol:
TFRC
LIAS
GAPDH
FDX1
FECH
ACO2
IRP2
ACTIN
IRP1

Figure S3

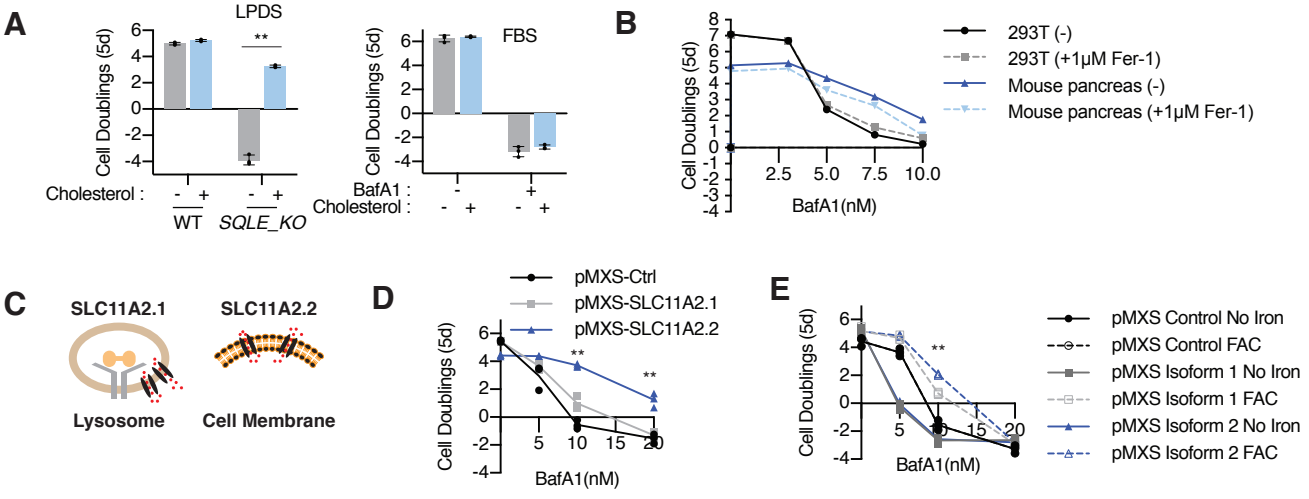
A
LPDS
FBS
Cell Doublings (5d)
**
Cholesterol :
BafA1 :
WT
SQLE_KO
B
293T (-)
293T (+1μM Fer-1)
Mouse pancreas (-)
Mouse pancreas (+1μM Fer-1)
BafA1(nM)
C
SLC11A2.1
SLC11A2.2
Lysosome
Cell Membrane
D
pMXS-Ctrl
pMXS-SLC11A2.1
pMXS-SLC11A2.2
BafA1(nM)
E
pMXS Control No Iron
pMXS Control FAC
pMXS Isoform 1 No Iron
pMXS Isoform 1 FAC
pMXS Isoform 2 No Iron
pMXS Isoform 2 FAC
BafA1(nM)

Figure S4

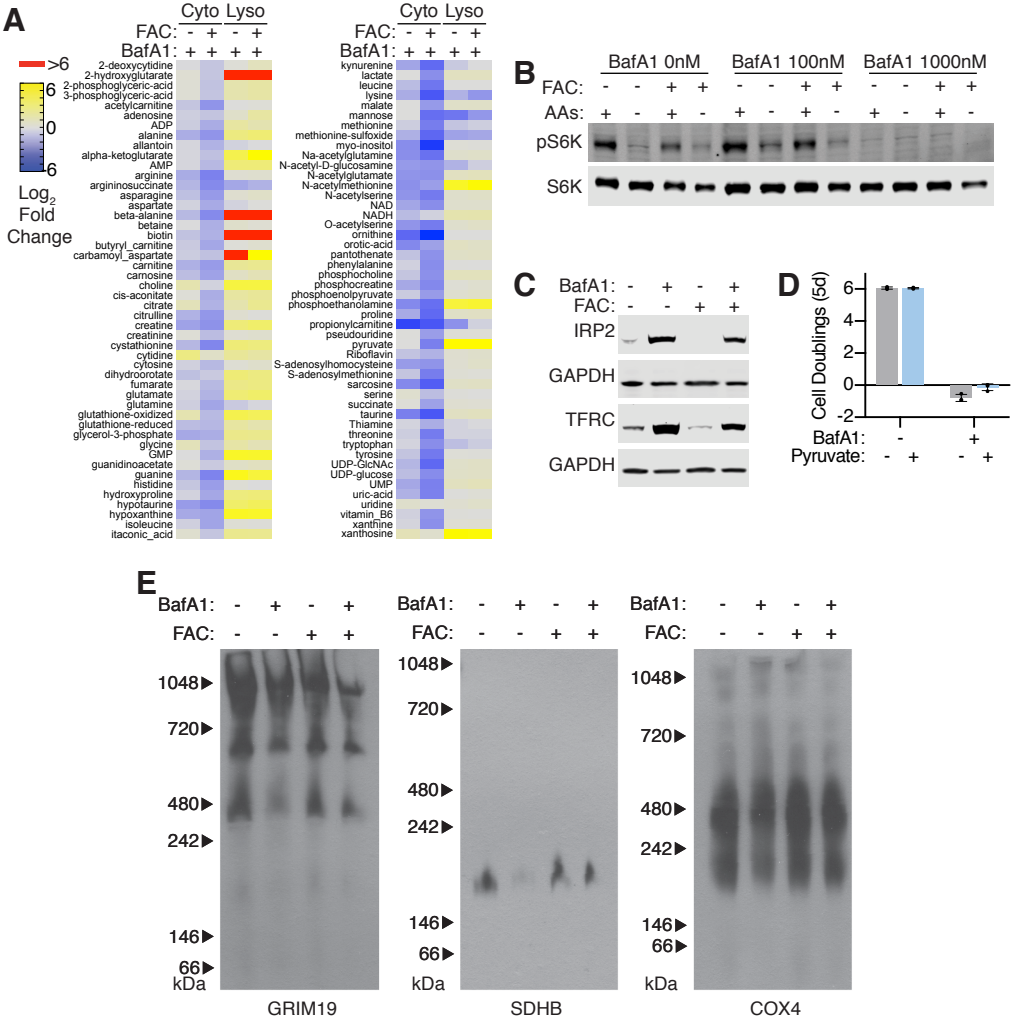
A
Cyto Lyso
FAC: - + - +
BafA1: + + + +
>6
6
0
6
Log2 Fold Change
2-deoxycytidine
2-hydroxyglutarate
2-phosphoglyceric-acid
3-phosphoglyceric-acid
acetylcarnitine
adenosine
ADP
alanine
allantoin
alpha-ketoglutarate
AMP
arginine
argininosuccinate
asparagine
aspartate
beta-alanine
betaine
biotin
butyryl_carnitine
carbamoyl_aspartate
carnitine
carnosine
choline
cis-aconitate
citrate
citrulline
creatine
creatinine
cystathionine
cytidine
cytosine
dihydroorotate
fumarate
glutamate
glutamine
glutathione-oxidized
glutathione-reduced
glycerol-3-phosphate
glycine
GMP
guanidinoacetate
guanine
histidine
hydroxyproline
hypotaurine
hypoxanthine
isoleucine
itaconic_acid
kynurenine
lactate
leucine
lysine
malate
mannose
methionine
methionine-sulfoxide
myo-inositol
Na-acetylglutamine
N-acetyl-D-glucosamine
N-acetylglutamate
N-acetylmethionine
N-acetylserine
NAD
NADH
O-acetylserine
ornithine
orotic-acid
pantothenate
phenylalanine
phosphocholine
phosphocreatine
phosphoenolpyruvate
phosphoethanolamine
proline
propionylcarnitine
pseudouridine
pyruvate
Riboflavin
S-adenosylhomocysteine
S-adenosylmethionine
sarcosine
serine
succinate
taurine
Thiamine
threonine
tryptophan
tyrosine
UDP-GlcNAc
UDP-glucose
UMP
uric-acid
uridine
vitamin_B6
xanthine
xanthosine
B
BafA1 0nM
BafA1 100nM
BafA1 1000nM
FAC: - - + + - - + + - - + +
AAs: + - + - + - + - + - + -
pS6K
S6K
C
BafA1: - + - +
FAC: - - + +
IRP2
GAPDH
TFRC
GAPDH
D
Cell Doublings (5d)
6
4
2
0
-2
BafA1: - +
Pyruvate: - + - +
E
BafA1: - + - +
FAC: - - + +
1048
720
480
242
146
66
kDa
GRIM19
SDHB
COX4

Figure S5

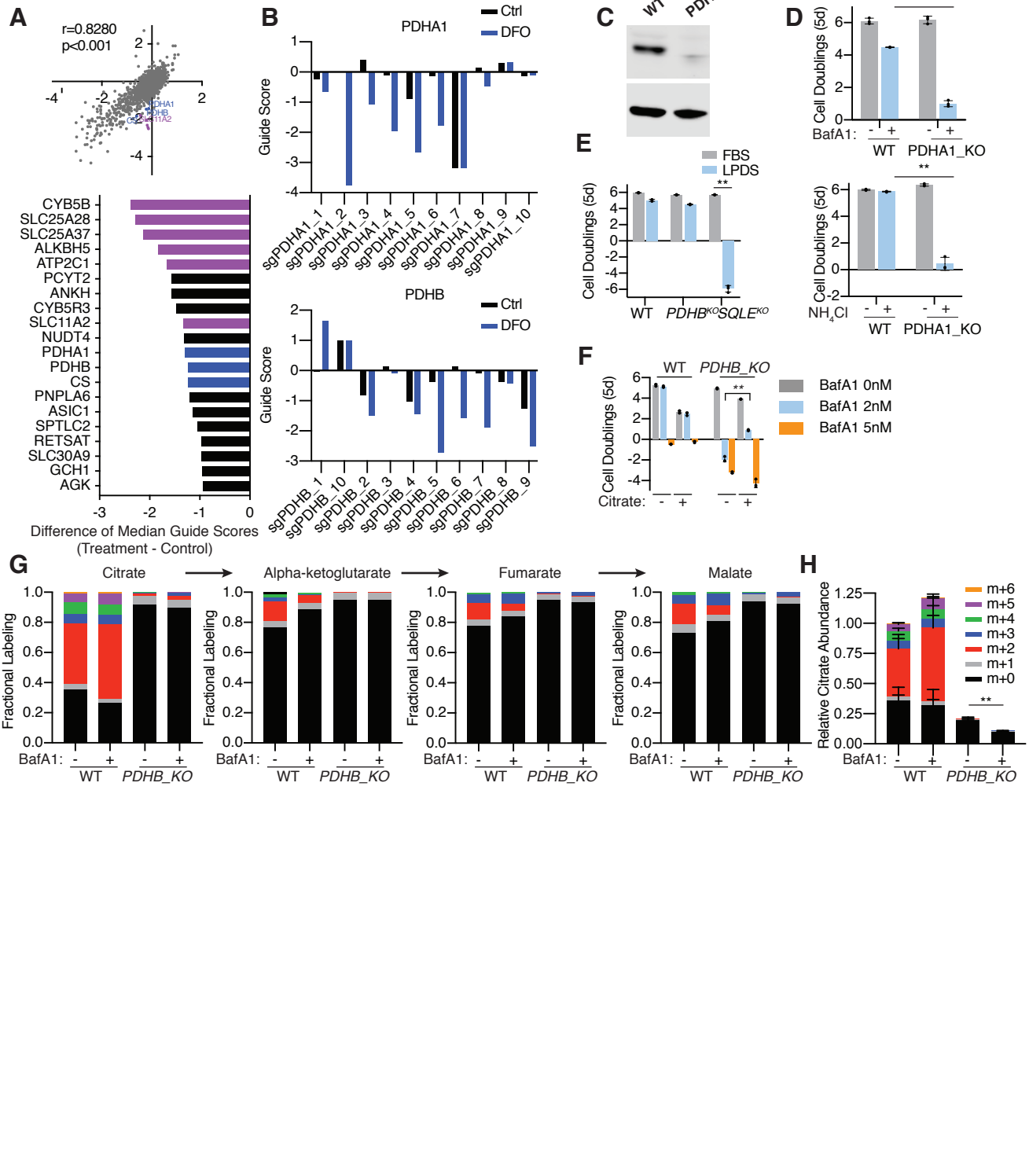
A
r=0.8280
p<0.001
PDHA1
PDHB
SLC11A2
CYB5B
SLC25A28
SLC25A37
ALKBH5
ATP2C1
PCYT2
ANKH
CYB5R3
SLC11A2
NUDT4
PDHA1
PDHB
CS
PNPLA6
ASIC1
SPTLC2
RETSAT
SLC30A9
GCH1
AGK
Difference of Median Guide Scores
(Treatment - Control)
B
PDHA1
Ctrl
DFO
Guide Score
sgPDHA1_1
sgPDHA1_2
sgPDHA1_3
sgPDHA1_4
sgPDHA1_5
sgPDHA1_6
sgPDHA1_7
sgPDHA1_8
sgPDHA1_9
sgPDHA1_10
PDHB
Ctrl
DFO
Guide Score
sgPDHB_1
sgPDHB_10
sgPDHB_2
sgPDHB_3
sgPDHB_4
sgPDHB_5
sgPDHB_6
sgPDHB_7
sgPDHB_8
sgPDHB_9
C
WT
PDHB^KO
D
Cell Doublings (5d)
BafA1:
WT
PDHA1_KO
E
FBS
LPDS
Cell Doublings (5d)
WT
PDHB^KO SQLE^KO
NH4Cl
WT
PDHA1_KO
F
WT
PDHB_KO
Cell Doublings (5d)
BafA1 0nM
BafA1 2nM
BafA1 5nM
Citrate:
G
Citrate
Alpha-ketoglutarate
Fumarate
Malate
Fractional Labeling
BafA1:
WT
PDHB_KO
H
Relative Citrate Abundance
m+6
m+5
m+4
m+3
m+2
m+1
m+0
BafA1:
WT
PDHB_KO

Figure S6

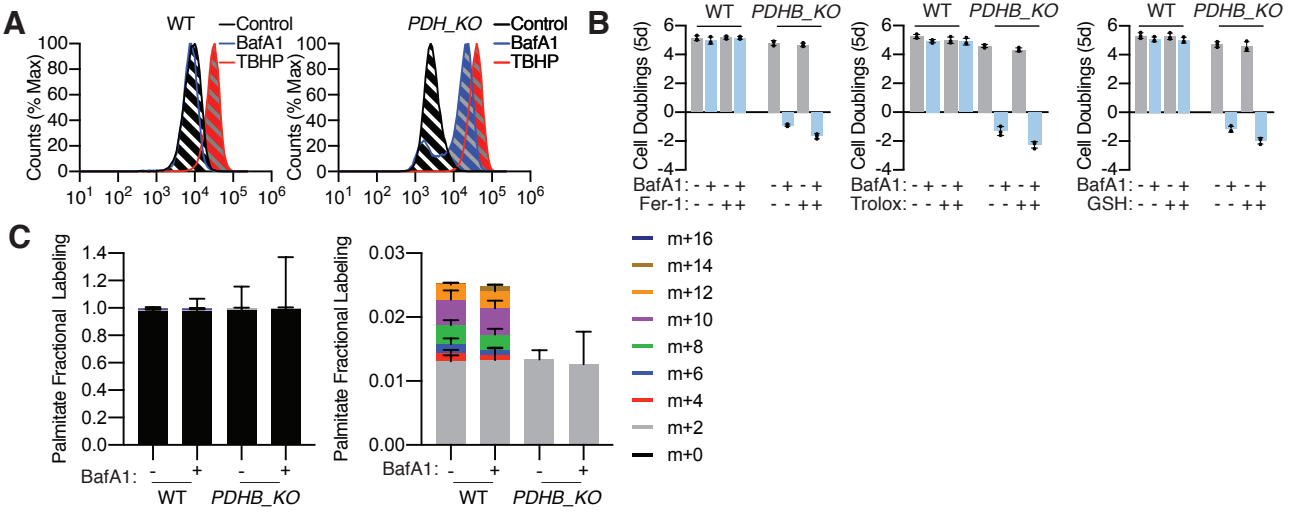
A
WT
Control
BafA1
TBHP
PDH_KO
Control
BafA1
TBHP
Counts (% Max)
B
WT
PDHB_KO
Cell Doublings (5d)
BafA1:
Fer-1:
Trolox:
GSH:
C
Palmitate Fractional Labeling
BafA1:
WT
PDHB_KO
m+16
m+14
m+12
m+10
m+8
m+6
m+4
m+2
m+0